

# Nonlinear Response Properties of Ultralarge Hyperpolarizability Twisted $\pi$ -System Donor–Acceptor Chromophores. Dramatic Environmental Effects on Response

Eric C. Brown, Tobin J. Marks,\* and Mark A. Ratner\*

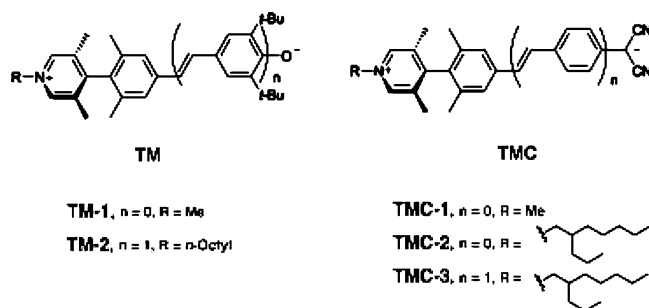
Department of Chemistry, Northwestern University, 2145 Sheridan Road, Evanston, Illinois 60208-3113

Received: March 29, 2007; In Final Form: August 22, 2007

State-average complete active space self-consistent field (SA-CASSCF) calculations are performed on the energetically lowest two electronic states of a novel alkyl-substituted 4-quinopyran twisted  $\pi$ -system electro-optic chromophore. In the gas phase, the ground-state electronic configuration is diradicaloid (**D**), and the first excited state is zwitterionic (**Z**). When an external dipolar field is applied to simulate polar solvation, the relative energies of **D** and **Z** are dramatically perturbed. At sufficient field strengths, the relative ordering of the states is inverted so that **Z** becomes the ground state. As the energy difference between the **D** and **Z** states falls, the magnitudes of the longitudinal static polarizability ( $\alpha$ ) and hyperpolarizability ( $\beta$ ) increase appreciably—in certain cases, by 2 orders of magnitude. These computational results are interpreted and supported by qualitative state correlation diagrams constructed from qualitative molecular orbital theory and are in agreement with recent experimental results on twisted  $\pi$ -system electro-optic chromophores (Kang, H. et al. *J. Am. Chem. Soc.* **2007**, *129*, 3267). The computational results also suggest that changing the environmental polarity is a promising strategy for tuning  $\alpha$  and  $\beta$  in such types of chromophores, which experimentally exhibit large nonlinear optical response.

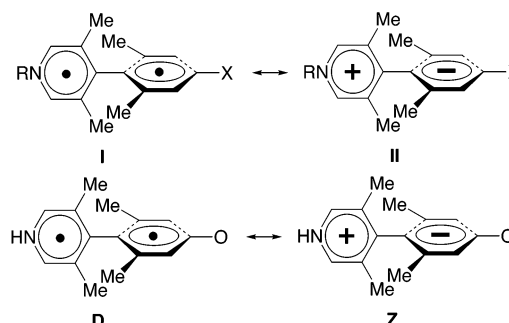
## 1. Introduction

A new class of “twisted  $\pi$ -system” donor–acceptor chromophores (tictoid and twisted intramolecular charge-transfer; **TM** and **TMC** below) that exhibit exceptionally large molecular nonlinear optical response was recently reported from this laboratory.<sup>1–4</sup>



Molecules with this “twisted” structural motif are of interest because of their potential applications in areas such as optical computing and telecommunications, signal processing, and data reconstruction.<sup>5–7</sup> Such organic-based materials have a number of attractive qualities versus inorganic materials, such as structural flexibility, optical transparency, low dielectric constants, and compatibility to the vast library of synthetic organic knowledge for their synthesis and derivatization.<sup>8–12</sup> Unlike inorganic crystals such as  $\text{LiNbO}_3$ , tictoid chromophores have closely lying electronic states,<sup>1,13,14</sup> and it is therefore possible that their large response properties may approach the “fundamental quantum limit” that has recently been proposed for organic-based materials.<sup>15,16</sup>

A strong dependence of tictoid chromophore hyperpolarizability ( $\beta$ ) upon the inter-ring torsional angle ( $\theta$ ) was predicted computationally,<sup>1</sup> and these predictions are generally supported by the experimental measurements of the molecular nonlinear susceptibility (molecular hyperpolarizability) via electric field-induced second harmonic generation (EFISH).<sup>3,4</sup> In an effort to better understand the approximations made in the original work of Albert et al.,<sup>1</sup> which predicted the sharp torsional angular dependence of  $\beta$ , Keinan et al. performed multireference configuration interaction (CI), with intermediate neglect of differential overlap (MRD-CI/INDO) calculations,<sup>13</sup> which are in qualitative agreement with the early work.<sup>1</sup> More recently, Isborn et al. performed large complete active space self-consistent field (CASSCF) calculations on model tictoid system **I/II** ( $R = \text{Me}$  and  $X = \text{O}$ ) and showed that the ground state singlet wave function at the fully twisted  $\theta = 90^\circ$  degree geometry is actually a diradical (**D**), with a zwitterionic state (**Z**) being only slightly higher in energy.<sup>14</sup> These states were argued to be analogous to the lowest states of the more elaborate (but experimentally realized) chromophore classes **TM** and **TMC** above.



\* Corresponding author. E-mail: t-marks@chem.northwestern.edu (T.J.M.); ratner@chem.northwestern.edu (M.A.R.).

Indeed, this is the *a priori* expected result because, in the gas phase, the charge separation in the zwitterionic state is energetically unfavorable for electrostatic reasons. The computed  $\beta$  of the diradicaloid state from these high-level calculations was reported to be orders of magnitude smaller than the  $\beta$  reported in the previous theoretical work. Although the  $\beta$  computed from large CASSCF calculations would seem to be more reliable, these calculations<sup>14</sup> are in apparent contradiction to the fact that  $\beta$  is very large when measured using EFISH experiments.<sup>3,4</sup> Isborn et al. noted that their calculations neglected any effect that solvation might have on the chromophore electronic structure.<sup>14</sup> Indeed, changes in the molecular hyperpolarizability are known to be intimately associated with the changes in the energy differences between the electronic states.<sup>17–19</sup>

In our previous work,<sup>3,4</sup> we observed a large dependence of the EFISH-derived  $\beta$  on the particular solvent used in the experiment. For example, the  $\beta$  of **TMC-3** decreases 4-fold upon changing the solvent from  $\text{CH}_2\text{Cl}_2$  to dimethylformamide (DMF).<sup>3,4</sup> Although we reported initial computational results that generally supported the solvation trends, the computational methods employed pragmatic but nonideal approximations. In the present study, we report a more detailed analysis of the potential energy surfaces of a tictoid chromophore employing the **D/Z** system as a model, and examine how electronic structure changes when subjected to a polarizing environment, such as an external applied field or polar solvent. In achieving this, we also report the results of high-level CASSCF calculations that support our more qualitative model. Finally, we show that the computed  $\beta$  can be orders of magnitude larger in certain dielectric media than it is in the gas phase, because the state ordering changes entirely.

## 2. Computational Methodology

Our approach to understanding  $\beta$  depends on how well we understand the quantities that determine  $\beta$ . Although qualitative theory can provide certain answers based on intuition and symmetry arguments, *ab initio* calculations are required for a more quantitative description. Motivated by the related work of others,<sup>20–32</sup> we set out with the goal of assessing with quantitative theory how  $\beta$  depends on twist angle  $\theta$  and also on the polarity of the environment.

**2.1. Response Properties.** We begin by recalling the established relationship between the (static) linear polarizability response  $\alpha$  or the nonlinear response  $\beta$  and quantities that can be determined from quantum chemistry calculations. Particularly useful relations come from the static ( $\omega = 0$ ), two-state approximations of Oudar and Chemla<sup>17</sup> to the “sum-over-states” (SOS) representations of Orr and Ward:<sup>33</sup>

$$\alpha_{\text{SOS}}(\omega = 0) \propto \frac{M_{\text{ge}}^2}{E_{\text{ge}}} \quad (1)$$

$$\beta_{\text{SOS}}(\omega = 0) \propto \frac{\mu_{\text{ge}} M_{\text{ge}}^2}{E_{\text{ge}}^2} \quad (2)$$

where  $\mu_{\text{ge}} = \mu_{\text{g}} - \mu_{\text{e}}$  represents the difference in dipole moments of the first excited state (e) and the ground state (g),  $M_{\text{ge}}$  is the transition dipole integral between the ground and excited states, and  $E_{\text{ge}} = E_{\text{g}} - E_{\text{e}}$  is the energy difference between the states.

In general, it is inconvenient to evaluate  $\alpha$  and  $\beta$  quantitatively from the SOS expressions because a large number of excited states (e) must be summed for convergence.<sup>34</sup> Another approach is more useful for quantitative evaluation of response properties

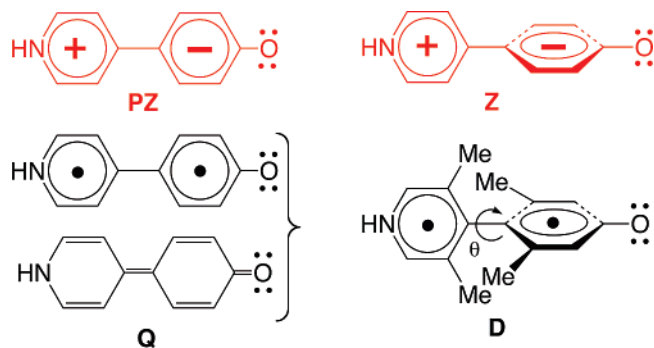


**Figure 1.** Valence bond description of the lowest electronic states of chromophores **I/II** where  $X = \text{O}$ ,  $R = \text{Me}$ , and  $R' = \text{H}$ . See text for the meaning of each label. For clarity, the  $o,o',o'',o'''$ -methyl groups are shown explicitly only on **D** at  $\theta = 90^\circ$ ; however these groups are present in the other resonance structures.

$\alpha$  and  $\beta$  in the static limit. The response of the energy to an applied external field can be written schematically as the Taylor series expansion<sup>9,10</sup>

$$-\frac{\partial E}{\partial F} = \mu = \mu_0 + \alpha F + \frac{1}{2}\beta FF + \dots \quad (3)$$

which leads to the derivative expressions

$$\alpha = \left. \frac{\partial \mu}{\partial F} \right|_{F=0} \quad (4)$$

$$\beta = \left. \frac{\partial^2 \mu}{\partial F^2} \right|_{F=0} \quad (5)$$

In this study, we employ the standard two-point (for  $\alpha$ ) and three-point (for  $\beta$ ) finite dipole difference formulas ( $\Delta F = 0.0001$  a.u.) to evaluate numerically  $\alpha$  and  $\beta$  shown in eqs 4 and 5; this is often called the finite-field (FF) approach.<sup>14</sup> We compute only the  $\alpha_{zz}$  and  $\beta_{zzz}$  components; these are the quantities that generally lead to practical nonlinear optical response properties for these push–pull-type chromophores. To understand qualitatively how the response properties change as a result of perturbations, we complement the high-level CASSCF/FF calculations with qualitative arguments based on eqs 1 and 2.

**2.2. Wave Functions.** Differing slightly from previous work,<sup>1,13,14</sup> we chose our **TC** with  $X = \text{O}$ , and  $R = \text{H}$  (rather than  $R' = \text{Me}$ ) as the model system for compounds such as **Ia** and **Ib**. At twist angles near  $\theta = 90^\circ$ , the lowest two states are diradicaloid (**D**) and zwitterionic (**Z**) (Figure 1).<sup>1,13,14</sup> Although other methods for describing diradicaloid states exist,<sup>35</sup> it is known that CASSCF (or CAS) theory<sup>36</sup> provides a theoretically sound framework for the description of both of these theoretically interesting states (**D** and **Z**). Since CAS is a type of CI calculation, CAS calculations are well-suited for describing excited states.

The selection of the “active space” in CAS calculations is not unique. A simple two-electron-in-two-orbital (CAS(2,2)) wave function provides a minimal description for a singlet diradical (**D**); likewise, two electrons in two orbitals can describe each of the one-electron excitations from **D** to form **Z**. Following Isborn et al., we construct an active space that encompasses the 14  $\pi$  electrons in 13  $\pi$  molecular orbitals: the CAS(14,13) wave function.<sup>14</sup> The (nominal) highest occupied molecular orbital (HOMO) and lowest unoccupied molecular orbital (LUMO) natural orbitals are shown pictorially in Figure 2.

Isborn et al. employed the more traditional single-state CASSCF (SS-CAS) computational approach in their evaluation

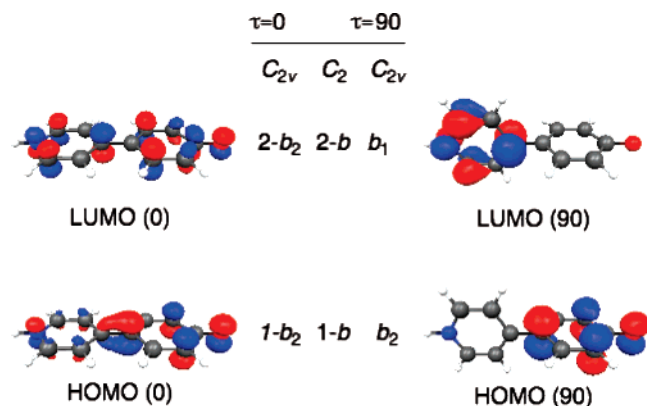


**Figure 2.** Pictorial representation of the natural orbitals of the (nominal) HOMO and LUMO in the active space of the SA-CAS(14,13) calculations.

of the response properties of **I/II**.<sup>14</sup> Since such SS-CAS calculations optimize to the best possible orbitals and CI coefficients for a particular state, they can be considered to be the best representation of that particular state. However, this type of calculation becomes problematic when other states are close in energy. In addition, in order to compute state interaction terms such as the transition dipole moment ( $M_{ge}$ ), one must go through a biorthogonalization process,<sup>37</sup> which is computationally arduous for molecules with such large active spaces. These issues can be circumvented by using a state-average CASSCF calculation (SA-CAS).<sup>38</sup> Therefore, the results reported here have been obtained with the two-state SA-CAS(14,13) level of theory, with equal weights for the ground and excited states.

For consistency with previous work and for reasons of tractability, we employ a 6-31G\*\* basis set for all calculations.<sup>39,40</sup> We note that the basis set is much smaller than the large, diffuse basis sets (e.g., aug-cc-pVTZ) that are necessary to accurately predict response properties. Although we desired to perform simulations with larger basis sets, our efforts were limited by (1) the sheer number of integrals that must be stored to the disk as the basis set is enlarged and (2) linear dependencies within the large basis set, which make it difficult to precisely converge the wave functions with the same number of basis functions over a range of torsional angles  $\theta$ .

Because of the small basis set, the computational results for  $\alpha$  and  $\beta$  must not be considered quantitatively, but rather they should be interpreted semiquantitatively. In particular, we are interested in how the sign, magnitude, and local maxima change with respect to changing the interphenyl torsional angle and the strength of a longitudinally applied field.

Geometries were optimized to both the lowest restricted Hartree–Fock (RHF) and the B3LYP<sup>41,42</sup> gas-phase state for a range of constrained torsional angles  $\theta$ . Both the RHF and the B3LYP densities resemble the **Z** state (as determined by the dipole moment), and they do not have the freedom to express the **D** state. Therefore, geometry optimizations inevitably favor the **Z** state over the **D** state. As we will show, the **Z** state and its geometry are probably the best for describing TCs in a polar solvent, because solvation selectively stabilizes the **Z** state relative to the **D** state. We discuss the differences in optimization to **D** or **Z** structures in section 4.3.

SA-CAS-evaluated response properties have similar features at both the RHF-optimized and B3LYP-optimized geometries, but, as expected,<sup>43</sup> they differ somewhat in their precise magnitudes. Since our interpretation of both sets of results are the same, we show the RHF results in the manuscript, and provide analogous B3LYP results in the Supporting Information.

Geometry optimizations were performed with the GAMESS package,<sup>44</sup> and FF perturbations were performed in  $C_2$  symmetry with the MOLCAS suite of ab initio quantum chemistry programs.<sup>38</sup>

**2.3. Effects of a Dielectric Medium.** We consider two simple continuum approaches to computing the effect of solvation. One choice for incorporating solvation effects is the integral equation formalism polarizable continuum model (IEF-PCM),<sup>45,46</sup> which forms an optimal enclosing surface around the solute molecule. Solvation effects were evaluated at the SA-CASSCF(14,13)/6-31G\*\* level of theory with the solute-conforming IEF-PCM model<sup>45,46</sup> as implemented in GAMESS.<sup>44</sup> As will be shown in the Results section, the principal effect of the solvent dielectric is to stabilize zwitterionic state **Z** relative to diradicaloid state **D**. These IEF-PCM calculations are extremely time-consuming because the calculations must be performed with no symmetry rather than in the  $C_2$  point group. Therefore, it is impractical to evaluate all of the points required to determine  $\beta$  and its dependence on torsional angle and solvent dielectric with this particular method.

Stabilization of the zwitterionic structure **Z** with respect to the diradical **D** can also be achieved by applying a simple dipole field applied along the longitudinal molecular axis defined by the interphenyl bond ( $z$  direction). This is reminiscent of the distributed point charges used by Marder and collaborators in developing the bond-length alternation (BLA) scheme for nonlinear chromophores.<sup>47</sup> It is computationally convenient that this perturbation preserves the overall  $C_2$  (or  $C_{2v}$  for  $\theta = 90^\circ$ ) symmetry of the system for all interphenyl torsional angles  $\theta$ . Importantly, this approach provides a way of determining the response properties via the FF scheme, as well as incorporating the stabilization of **Z** relative to **D**. With two simultaneously applied dipolar fields—(1) a large applied field (order of  $\Delta F = 0.001$  a.u.) that mimics the solvation effect and (2) a smaller field (order of  $\Delta F = 0.0001$  a.u.) that slightly perturbs the dipole moment of the lowest states of TC—we obtain  $\alpha_{zz}$  and  $\beta_{zzz}$  in a particular “solvent medium.”

### 3. Results

#### 3.1. Potential Energy Surfaces of Twisted Chromophores.

As the solvent dielectric constant or dipole field strength is increased, structures **D** and **Z** fall in energy because they experience some degree of solvation. From eqs 1 and 2, only the energy difference between states is important, so when presenting the energy differences, we set as the zero of energy the ground state at the  $\theta = 90^\circ$  geometry for a particular applied field or solvent dielectric constant. Figure 3 shows the potential energy surfaces of the two twisted chromophore lowest states as a function of applied field strength and torsional angle  $\theta$ . In the gas phase, the ground state surface can be described as a double-well potential centered at  $\theta = 90^\circ$  and with minima at  $\theta = 55^\circ$  and  $\theta = 125^\circ$ . However, applying an external field dramatically changes the shape of the ground-state potential energy surface. Beyond an applied field strength of 0.002 a.u., the potential energy surface begins to flatten out, although the double-well character remains perceptible. The first excited-state is roughly parabolic and centered about  $\theta = 90^\circ$  at all applied field strengths.

Also shown in Figure 3 is the energy difference between the ground state and the first excited state ( $E_{ge}$ ). Near an applied field of 0.002 a.u. and  $\theta = 90^\circ$ , the difference between the ground state and the first excited state practically vanishes, as shown in Figure 3. It is desirable to establish a relationship between the stabilization provided by the applied field and the



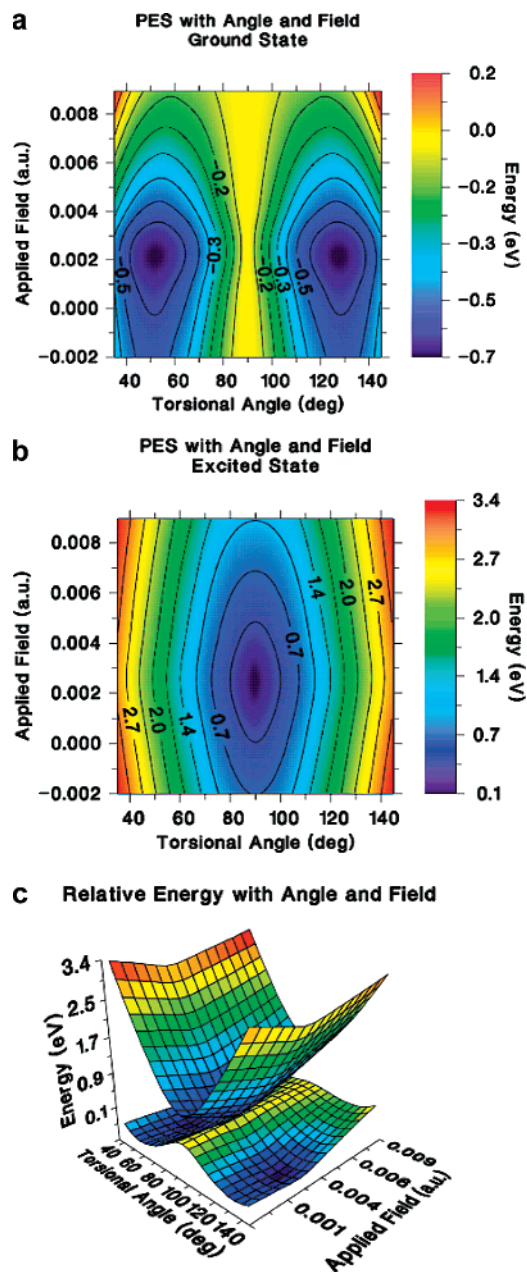


**Figure 3.** Potential energy surfaces (PESs) of the ground (a) and excited (b) states of TC with torsional angle relative to the energy of the ground state at  $\theta = 90^\circ$  at a particular applied field. In panel c, the surfaces shown in panels a and b are combined and employ the same color values for their respective surfaces.

solvent continuum model. At  $\theta = 90^\circ$ , an IEF-PCM calculation with a solvent dielectric constant between 2.0 and 3.0 also leads to the (accidental) degeneracy of the ground and excited-state energies. Therefore, we estimate that the field strength of 0.002 a.u. is equivalent to the scenario where the solvent dielectric constant is  $\sim 3.0 \epsilon_0$ .

This result is significant, because most experimental characterization studies (e.g., EFISH) of tictoid chromophores are performed in solvents with a significantly higher dielectric constant<sup>4</sup> and even a solid-state polymer constructed from tictoid building blocks would have a dielectric constant of at least 4.<sup>48</sup> These results argue for a narrow applicability of gas-phase computational results for twisted chromophores<sup>1,13,14</sup> in understanding the experimental properties of such molecules in typical useful solvents.

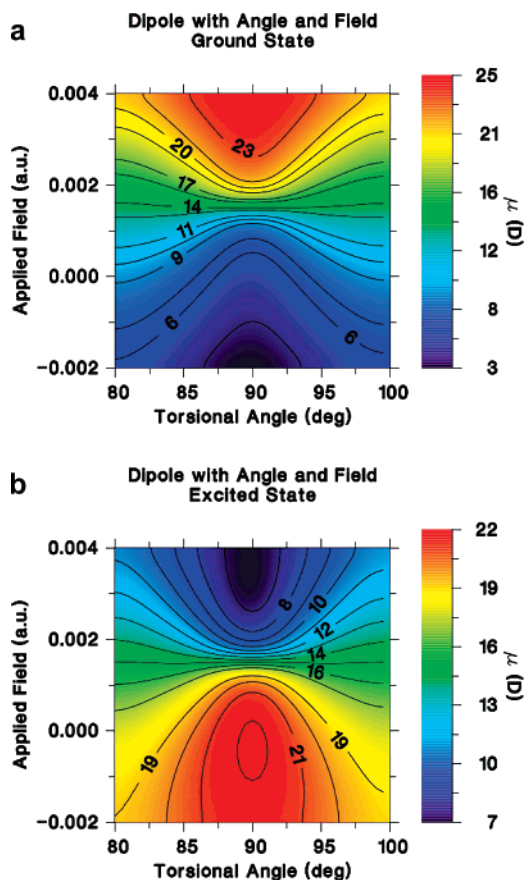


**Figure 4.** Dipole moments of the ground (a) and excited (b) states of TC as a function of torsional angle ( $\theta$ ) at a particular applied field.

**3.2. Dipole Moments.** The dipole moment of each state provides information as to which valence bond structure, **D** or **Z**, should be ascribed to a particular state. Because of its large charge separation, the zwitterionic structure **Z** should have a larger dipole moment than **D**. The dipole moment of the lowest two electronic states of TC as a function of torsional angle  $\theta$  and the applied field can be found in Figure 4. Considering only  $\theta = 90^\circ$  at applied field strengths below 0.002 a.u. (or  $\epsilon_0 = 3$  in the solvent dielectric model, *vide supra*), the dipole moment of the ground state is lower than the dipole moment of the excited state, suggesting that the ground state is **D** and the first excited state is **Z**, in agreement with the results found by Isborn et al.<sup>14</sup> It is perhaps noteworthy that the computed ground state of TC (near  $\theta = 90^\circ$ ) in apolar environments is actually a triplet state,<sup>13</sup> in agreement with simple ideas based on Hund's rule. As shown in Figure 4, increasing the applied field beyond 0.002 a.u. reverses the energy ordering of **D** and **Z**. Beyond an applied field of 0.002 a.u., the dipole moment of the ground state is larger than the dipole moment of the first excited state, and so we label the ground state **Z** and the first excited state **D**.

**3.3. Nonlinear Response Properties.** In addition to providing a straightforward way to characterize each electronic state, the dipole moment and its various derivatives with respect to applied fields afford the response functions  $\alpha$  and  $\beta$  which are the central focus of this work. The static polarizability ( $\alpha$ ) and the static hyperpolarizability ( $\beta$ ) with respect to torsional angle and applied dipole field were plotted and are shown in Figure 5.

In agreement with earlier calculations,<sup>1,13,14</sup> the gas-phase  $\alpha$  and  $\beta$  values for TC have maxima away from  $\theta = 90^\circ$ . The present SA-CAS(14,13) calculations indicate that the maximum polarizability of TC is found at  $\theta = 80^\circ$ , with a value of  $95 \text{ \AA}^3$ . Although this value is larger than the polarizability previously

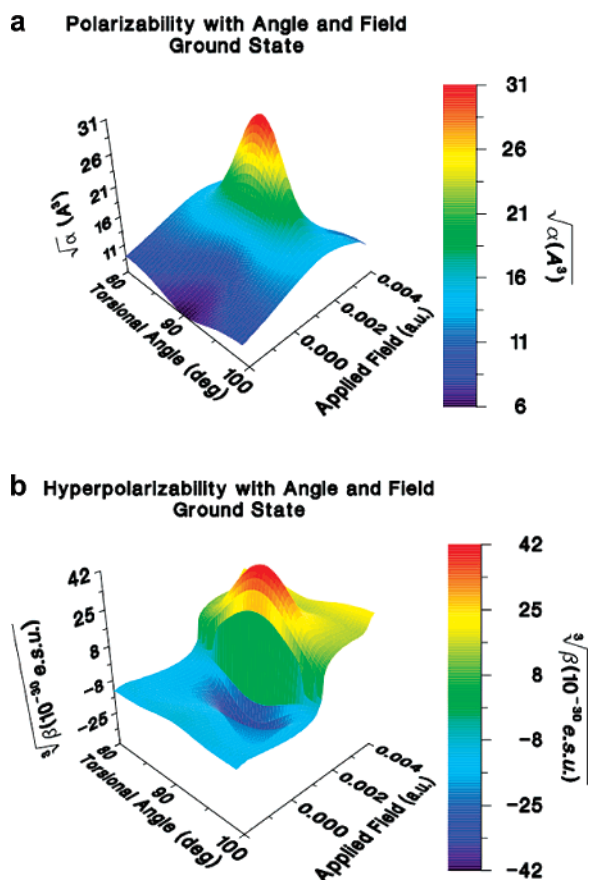


**Figure 5.** Response functions  $\alpha$  (a) and  $\beta$  (b) as a function of applied field and torsional angle. Because of the large differences in magnitude, the square root of  $\alpha$  and the cube root  $\beta$  of are shown for plotting clarity.

reported,<sup>14</sup> we note that we are only considering the  $\alpha_{zz}$  component of the polarizability, not “diluted” by averaging over the (likely smaller) elements of the total polarizability matrix. As **TC** is planarized, the polarizability converges upon a value of  $47 \text{ \AA}^3$ ,<sup>3</sup> in line with values reported for other donor–acceptor chromophores using several levels of computational sophistication.<sup>43</sup> The gas phase  $\beta$  of **TC** has a maximum at  $\theta = 80^\circ$ , with a  $\beta_{zzz}$  value of  $-1800 (10^{-30} \text{ esu})$ . Again, this finding is in agreement with the magnitudes and signs of the values found by Isborn et al.,<sup>14</sup> although it is somewhat smaller than the values reported by Keinan et al.<sup>13</sup>

The plots of  $\alpha$  and  $\beta$  as a function of torsional angle and applied field (Figure 5) reveal several interesting trends. The magnitudes of these response properties can increase by orders of magnitude over their gas-phase values if the applied field is such that the electronic states become proximate in energy (Figure 3). Even more surprising is that, upon approaching an applied field of  $0.002 \text{ a.u.}$ , the maxima of  $\alpha$  and  $\beta$  move from  $\theta = 80^\circ$  to  $\theta = 90^\circ$ . Beyond  $0.002$ , the maximum values of  $\alpha$  or  $\beta$  revert from  $\theta = 90^\circ$  back to  $\theta = 80^\circ$ . Finally, the sign of  $\beta$  changes from negative values below an applied field of  $0.002 \text{ a.u.}$  to positive values when the field is increased beyond this point of near-degeneracy, in agreement with experiment.<sup>3,4</sup> The remainder of this discussion is concerned with the origin of these trends.

#### 4. Discussion

The primary goal of this investigation is to evaluate computationally the nonlinear response,  $\beta$ , of a prototypical twisted  $\pi$ -electron chromophore (**TC**) as a function of environmental

polarity and molecular torsional angle  $\theta$ . From the approximate relationships between  $\alpha$  and  $\beta$  and computable properties of molecules (eqs 1 and 2), we attempt to explain the trends in  $\alpha$  and  $\beta$  as computed from eqs 4 and 5.

**4.1. Valence-Bond Description of the Lowest Energy States.** It is well-established from previous and the present calculations that the electronic structures of the lowest two states of **TC** ( $\theta = 90^\circ$ ) can be described as being predominantly diradicaloid (**D**) or zwitterionic (**Z**).<sup>13,14</sup> The diradical state (**D**) has been found computationally to be the singlet<sup>14</sup> gas-phase ground state of twisted chromophores **I/II** ( $\theta = 90^\circ$ ). The major difference between the resonance structures **D** and **Z** is their relative occupations of the pyridinium ring and phenoxide ring  $\pi$ -spaces.

From eq 2, because the terms  $(M_{ge})^2$  and  $E_{ge}$  are always positive (or zero), the sign of  $\mu_{ge}$  determines the sign of  $\beta$ . When **D** is the ground state and **Z** is the first excited state (applied fields  $< 0.0040 \text{ a.u.}$ ), the term  $\mu_{ge}$  is negative; hence,  $\beta$  is negative, as shown in Figure 5. Increasing the applied field beyond  $0.002 \text{ a.u.}$  stabilizes the **Z** state with respect to the energy of the **D** state. Therefore, the sign of  $\beta$  is positive because  $\mu_{ge}$  is positive. Figures 4 and 5 show that  $\mu_{ge}$  and  $\beta$  indeed have the same sign.

**4.2. Transition Moment between Lowest Electronic States.** The response properties  $\alpha$  and  $\beta$  also depend on the transition moment integral,  $M_{ge}$ . At  $\theta = 90^\circ$ , **TC** possesses  $C_{2v}$  symmetry, and this integral can be computed from symmetry considerations.<sup>49</sup> We first assign term symbols to the two lowest states. To assign state symmetries, we determine the symmetries and occupations of the MOs that comprise each state. Shown in Figure 2 are the “frontier” orbitals that are required for the minimal description of the lowest two electronic states of **TC** at  $\theta = 90^\circ$ .

From our SA-CAS calculations, we find that, at  $\theta = 90^\circ$  degrees, the CI coefficients and wave functions for each state can be roughly described as

$$\Psi_D \approx |\cdots b_2^1 b_1^1\rangle \approx |\mathbf{D}\rangle \quad (6)$$

$$\Psi_Z \approx |\cdots b_2^2 b_1^0\rangle \approx |\mathbf{Z}\rangle \quad (7)$$

where proper spin antisymmetrization is implied. The spatial characteristics and electronic occupations of the MOs (eqs 6 and 7) are easily associated with the valence-bond representation shown in Figure 1.

The state symmetries of the wave functions can thus be assigned:  $\Psi_D$  is  $A_2$ ;  $\Psi_Z$  has  $A_1$  symmetry. Then,  $\langle \Psi_D | \mu | \Psi_Z \rangle = 0$  because  $A_1 \times \mu \times A_2$  does not contain the totally symmetric representation. If **D** is the ground state (in agreement with the gas-phase calculations of Isborn et al.), then the excited state **Z** contributes nothing to the ground state **D** at  $\theta = 90^\circ$ . This explains, from qualitative theory, why the hyperpolarizability of gas phase **TC** is very small when  $\theta = 90^\circ$ , yet can be large at angles away from  $\theta = 90^\circ$ .<sup>1,13,14</sup>

What is puzzling about these results is that the SA-CAS-computed  $\alpha$  and  $\beta$  can have maxima at  $\theta = 90^\circ$ , depending on the applied field strength, although the transition moment  $M_{ge}$  is found (by both SA-CAS calculations and group theory) to be zero between **D** and **Z**, for all fields (eqs 1 and 2). We ascribe this discrepancy to the breakdown of eqs 1 and 2 when the states approach accidental degeneracy. Indeed, eqs 1 and 2 were derived from nondegenerate perturbation theory, and are likely pathological in this regime.<sup>33,17</sup> The trends predicted by eqs 1 and 2 are thus completely consistent with the SA-CAS results

in applied fields where the states are energetically well-separated.<sup>33,17</sup>

**4.3. Potential Energy Surfaces.** We have discussed only the effects of environmental polarity on the energies of the  $\theta = 90^\circ$  tictoid structure. We recall that the potential energy surface of the gas-phase ground state of **I/II** (Figure 3) is at a minimum near  $\theta = 50^\circ$ . Furthermore, there is a significant 0.5 eV energetic penalty associated with completely twisting the molecule from its minimum at  $\theta = 45^\circ$  to  $\theta = 90^\circ$ . A natural question arises: Can this particular twisted chromophore access the geometry region associated with the large nonlinear response, which is always a maximum between  $\theta = 80^\circ$  and  $90^\circ$ ?

As shown in Figure 3, increasing the applied field effects a significant change on the torsional potential energy surface of the ground state. Increasing the applied field to 0.002 a.u. deepens the double well ( $-0.7$  eV). However, further increasing the applied field strength leads to the virtual disappearance of the double-well minimum character. Because of these shallow minima, it is reasonable to suspect that the nuclear distribution can be spread over a larger range of torsional angles  $\theta$  when the environmental polarity is high. These computational results are supported by the experimental observation that the torsional angles in similar tictoids are between  $\theta = 80^\circ$  and  $90^\circ$ .<sup>4</sup>

In our previously reported calculations,<sup>4</sup> the double well minima were well pronounced at all applied field strengths. However, these calculations are different in two significant ways. First, these calculations treat the methyl group repulsions explicitly, whereas the previous calculations employed a model methyl potential.<sup>4</sup> Second, the present calculations were performed at the RHF-optimized geometry, whereas the previously reported calculations were performed at the diradicaloid, SA-CAS(4,3) optimized geometry of phase geometry. At all applied fields beyond 0.002 a.u., the ground-state wave function near  $\theta = 90^\circ$  is **Z**. Since the properties of the RHF wave function (e.g., dipole moment) strongly resemble the properties of **Z**, it is reasonable to suspect that the RHF geometry is more appropriate for describing the geometry of twisted chromophores that are in the solid state or solution.<sup>4</sup>

Planarization of the chromophore from  $\theta = 90^\circ$  toward  $0^\circ$  increases the contribution of the quinoidal form **Q** and decreases the contribution of **D** (Figure 1). In **Q**, it is possible to draw a resonance structure that places a double bond between the oxygen atom and its ipso carbon atom. The strength of this carbonyl  $\pi$  bond is a significant driving force for planarization away from  $\theta = 80$ – $90^\circ$ . It is possible that chromophore substituents that may not form such strong  $\pi$  bonds ( $-\text{C}(\text{CN})_2$ ) in **TM** and **TMC** will lead to structures that have equilibrium geometries closer to  $\theta = 80$ – $90^\circ$  degrees.<sup>4</sup> An additional strategy for realizing molecules with twist angles near this region of maximal  $\beta$  would be to annelate the molecule in order to “lock” it into a particular torsional configuration.

## 5. Conclusions

From high-level, multistate SA-CASSCF calculations, we have demonstrated that, for a prototypical tictoid chromophore, there is a dramatic change in the static linear response  $\alpha$  and the static nonlinear response  $\beta$  when subjected to a polar environment. From the SOS expressions (eqs 1 and 2), this can be understood as a manifestation of large solvent effects on the dipole moment and energy differences between the lowest states. In fact, these calculations predict that the state orderings change completely upon progressing from the gas phase where the ground state is diradicaloid, **D**, to a polar environment where the ground state is actually zwitterionic, **Z**. In applied fields

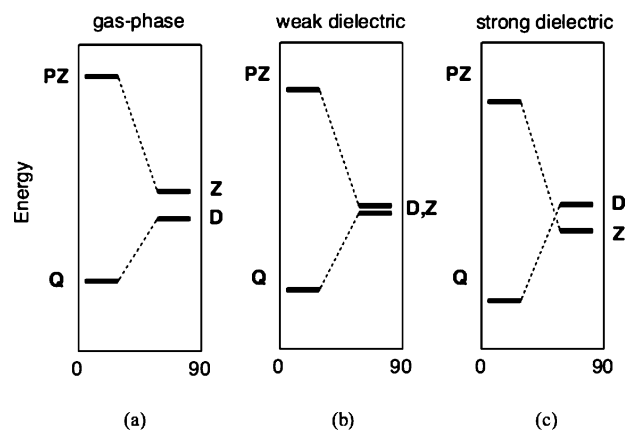


**Figure 6.** Qualitative state correlation diagrams as a function of twist angle  $\theta$  and increasing solvent polarity. Panel a represents the gas-phase picture, whereas panels b and c represent the state orderings as the environmental polarity is increased.

where the states cross, we predict extremely large static  $\alpha$  and  $\beta$  response, which can be 2 orders of magnitude larger than the computed gas-phase values.

We predict that the environmental polarity can be adjusted to give either a very large nonlinear response or a smaller nonlinear response. For example, increasing the applied field beyond 0.002 a.u. leads to a decrease in the computed  $\beta$  because the energy difference between **D** and **Z** starts to increase (eq 2). These results are in qualitative agreement with experimentally observed trends in similar chromophores such as **TMC**.<sup>3,4</sup>

Because the relevant states cross at certain applied fields (see Figure 6), the static, adiabatic picture presented here is a first approximation to the true dynamical description of the nonlinear response of these molecules. Indeed, nonadiabatic effects may alter the conclusions presented in this work. Further experimental and theoretical studies, aimed at probing the details of these several theoretical predictions, are underway in our laboratory.

**Acknowledgment.** We are grateful to DARPA/ONR (SP01P7001R-A1/N00014-00-C) and the NSF-Europe Program (DMR 0353831) for support of this research. All simulations were performed with a generous allotment of computer time provided by the National Energy Research Scientific Computing Center (NERSC). We thank D. Frattarelli, H. Kang, A. Fachetti, M. Sukharev, and G. Katz for helpful discussions.

**Supporting Information Available:** Response functions computed at the B3LYP-optimized geometries. This material is available free of charge via the Internet at <http://pubs.acs.org>.

## References and Notes

- (1) Albert, I. D. L.; Marks, T. J.; Ratner, M. A. *J. Am. Chem. Soc.* **1998**, *120*, 11174.
- (2) Kang, H.; Facchetti, A.; Stern, C. L.; Rheingold, A. L.; Kassel, W. S.; Marks, T. J. *Org. Lett.* **2005**, *7*, 3721.
- (3) Kang, H.; Facchetti, A.; Zhu, P. W.; Jiang, H.; Yang, Y.; Cariati, E.; Righetto, S.; Ugo, R.; Zuccaccia, C.; Macchioni, A.; Stern, C. L.; Liu, Z. F.; Ho, S. T.; Marks, T. J. *Angew. Chem., Int. Ed.* **2005**, *44*, 7922.
- (4) Kang, H.; Facchetti, A.; Jiang, H.; Cariati, E.; Righetto, S.; Ugo, R.; Zuccaccia, C.; Macchioni, A.; Stern, C. L.; Liu, Z.; Ho, S. T.; Brown, E. C.; Ratner, M. A.; Marks, T. J. *J. Am. Chem. Soc.* **2007**, *129*, 3267.
- (5) Dalton, L. *Adv. Polym. Sci.* **2002**, *158*, 1.
- (6) Dalton, L. R. *Pure Appl. Chem.* **2004**, *76*, 1421.
- (7) Zyss, J. *Chem. Phys.* **1999**, *245*, Preface.
- (8) Verbeist, T.; Houbrechts, S.; Kauranen, M.; Clays, K.; Persoons, A. *J. Mater. Chem.* **1997**, *7*, 2175.



- (9) Prasad, P. N.; Williams, D. J. *Introduction to Nonlinear Optical Effects in Molecules and Polymers*; Wiley: New York, 1991.
- (10) Chemla, D. S.; Zyss, J. *Nonlinear Optical Properties of Organic Molecules and Crystals*; Academic Press: New York, 1987.
- (11) Ratner, M. A. *Int. J. Quantum Chem.* **1992**, 43, 5.
- (12) Maroulis, G. *Atoms, Molecules, and Clusters in Electric Fields: Theoretical Approaches to the Calculation of Electric Polarizability*; Imperial College Press: London, 2006.
- (13) Keinan, S.; Zojer, E.; Bredas, J.-L.; Ratner, M. A.; Marks, T. J. *J. Mol. Struct.: THEOCHEM* **2003**, 633, 227.
- (14) Isborn, C. M.; Davidson, E. R.; Robinson, B. H. *J. Phys. Chem. A* **2006**, 110, 7189.
- (15) Tripathy, K.; Moreno, J. P.; Kuzyk, M. G.; Coe, B. J.; Clays, K.; Kelley, A. M. *J. Chem. Phys.* **2004**, 121, 7932.
- (16) Kuzyk, M. G. *J. Chem. Phys.* **2006**, 125, 154108.
- (17) Oudar, J. L.; Chemla, D. S. *J. Chem. Phys.* **1977**, 66, 2664.
- (18) Kanis, D. R.; Ratner, M. A.; Marks, T. J. *Chem. Rev.* **1994**, 94, 195.
- (19) Dehu, C.; Meyers, F.; Hendrickx, E.; Clays, K.; Persoons, A.; Marder, S. R.; Bredas, J. L. *J. Am. Chem. Soc.* **1995**, 117, 10127.
- (20) Agren, H.; Vahtras, O.; Koch, H.; Jorgensen, P.; Helgaker, T. *J. Chem. Phys.* **1993**, 98, 6417.
- (21) Mikkelsen, K. V.; Luo, Y.; Agren, H.; Jorgensen, P. *J. Chem. Phys.* **1994**, 100, 8240.
- (22) Fox, T.; Rösch, N. *Chem. Phys. Lett.* **1992**, 191, 33.
- (23) Bishop, D. M. *Int. Rev. Phys. Chem.* **1994**, 13, 21.
- (24) Bartkowiak, W. *Synth. Met.* **2000**, 109, 109.
- (25) Bartkowiak, W.; Lipkowski, P. *J. Mol. Model.* **2005**, 11, 317.
- (26) Bartkowiak, W.; Zalesny, R.; Kowal, M.; Leszczynski, J. *Chem. Phys. Lett.* **2002**, 362, 224.
- (27) Jacquemin, D.; Assfeld, X.; Perpete, E. A. *J. Mol. Struct.: THEOCHEM* **2004**, 710, 13.
- (28) Lipinski, J.; Bartkowiak, W. *Chem. Phys.* **1999**, 245, 263.
- (29) Wang, C. K.; Wang, Y. H.; Su, Y.; Luo, Y. *J. Chem. Phys.* **2003**, 119, 4409.
- (30) Willetts, A.; Rice, J. E. *J. Chem. Phys.* **1993**, 99, 426.
- (31) Zhu, W. H.; Wu, G. S.; Jiang, Y. S. *Int. J. Quantum Chem.* **2002**, 86, 347.
- (32) Zuliani, P.; Delzoppo, M.; Castiglioni, C.; Zerbi, G.; Marder, S. R.; Perry, J. W. *J. Chem. Phys.* **1995**, 103, 9935.
- (33) Orr, B. J.; Ward, J. F. *Mol. Phys.* **1971**, 20, 513.
- (34) Kanis, D. R.; Marks, T. J.; Ratner, M. A. *Int. J. Quantum Chem.* **1992**, 43, 61.
- (35) Nakano, M.; Kishi, R.; Nakagawa, N.; Ohta, S.; Takahashi, H.; Furukawa, S.; Kamada, K.; Ohta, K.; Champagne, B.; Botek, E.; Yamada, S.; Yamaguchi, K. *J. Phys. Chem. A* **2006**, 110, 4238.
- (36) Schmidt, M. W.; Gordon, M. S. *Annu. Rev. Phys. Chem.* **1998**, 49, 233.
- (37) Malmqvist, P. A.; Roos, B. O. *Chem. Phys. Lett.* **1990**, 155, 189.
- (38) Karlstrom, G.; Lindh, R.; Malmqvist, P. A.; Roos, B. O.; Ryde, U.; Veryazov, V.; Widmark, P. O.; Cossi, M.; Schimmelpfennig, B.; Neogrady, P.; Seijo, L. *Comput. Mater. Sci.* **2003**, 28, 222.
- (39) Hehre, W. J.; Ditchfield, R.; Pople, J. A. *J. Chem. Phys.* **1972**, 56, 2257.
- (40) Harihan, P. C.; Pople, J. A. *Theor. Chim. Acta* **1973**, 28, 213.
- (41) Becke, A. D. *J. Chem. Phys.* **1993**, 98, 5648.
- (42) Lee, C.; Yang, W.; Parr, R. G. *Phys. Rev. B* **1988**, 37, 785.
- (43) Kirtman, B.; Champagne, B. *Int. Rev. Phys. Chem.* **1997**, 16, 389.
- (44) Schmidt, M. W.; Baldrige, K. K.; Boatz, J. A.; Elbert, S. T.; Gordon, M. S.; Jensen, J. H.; Koseki, S.; Matsunaga, N.; Nguyen, K. A.; Su, S. J.; Windus, T. L.; Dupuis, M.; Montgomery, J. A. *J. Comput. Chem.* **1993**, 14, 1347.
- (45) Cancès, E.; Mennucci, B.; Tomasi, J. **1997**, 107, 3032.
- (46) Mennucci, B.; Cancès, E.; Tomasi, J. *J. Phys. Chem. B* **1997**, 101, 10506.
- (47) Meyers, F.; Marder, S. R.; Pierce, B. M.; Bredas, J. L. *J. Am. Chem. Soc.* **1994**, 116, 10703.
- (48) Lide, D. R. *CRC Handbook of Chemistry and Physics*; CRC Press: Boca Raton, FL, 2004.
- (49) Cotton, F. A. *Chemical Applications of Group Theory*; John Wiley: New York, 1990.